Materials Research Bulletin 84 (2016) 267–272

Contents lists available at ScienceDirect

Materials Research Bulletin

journal homepage: www.elsevier.com/locate/matresbu

Preparation of curcumin loaded mesoporous silica nanoparticles: Determining polarizability inside the mesopores

Digambara Patra[a,*], Didem Şen Karaman[b,c], Diti Desai[b], Elsy El Khoury[a], Jessica M. Rosenholm[b,*]

[a] Department of Chemistry, American University of Beirut, Beirut, Lebanon
[b] Pharmaceutical Sciences Laboratory, Faculty of Science and Engineering, Åbo Akademi University, Turku, Finland
[c] Laboratory for Physical Chemistry, Faculty of Science and Engineering, Åbo Akademi University, Turku, Finland

ARTICLE INFO

Article history:
Received 26 March 2016
Received in revised form 2 July 2016
Accepted 7 August 2016
Available online 8 August 2016

Keywords:
A. Microporous materials
A. Nanostructures
B. Optical properties
C: X-ray diffraction
C. Transmission electron microscopy (TEM)
D. Surface properties

ABSTRACT

Curcumin loaded mesoporopus silica nanoparticles (MSN) with various surface modifications have been prepared. SEM images indicate particle sizes in the range 200–300 nm. Various percentages of curcumin were successfully loaded within the nanoparticles, whereby the resultant loading degree increases linearly with the initial curcumin concentration. The polarizability inside the pores of MSN can be measured by using curcumin as fluorescence probe, which is critical since this cannot usually be easily reached using more conventional characterization methods. It was found that the polarizability value inside the pore is about 0.32, suggesting a solvent environment similar to methanol/ethanol. However, increase in the accumulated curcumin amount on the MSN reduces the energy gap between ground and excited state that saturated at higher curcumin loading due to homo energy transfer between the molecules. Surface modification of MSN also influences the spectral properties of curcumin due to change in pH, especially local accumulation of protons.

1. Introduction

Mesoporous silica nanoparticles (MSN) have drawn intense interest for various applications in materials sciences, catalysis and biomedical applications [1–4]. The exclusive properties of MSN are due to their narrow pore size distribution, high specific surface area and pore volume, tunable pore sizes and structures etc. Various methods including fast self-assembly, soft and hard templating, modified Stöber method, aerogel approaches etc. have been in practice applied to fabricate MSN [5–7]. Surface functionalization of such materials has further found to promote applications in e.g. base catalyzed reactions, post-synthesis of functionalization, and heavy metal sorbents [8–11]. Many approaches have been developed for flexible, versatile and straightforward surface functionalization of MSN with varying degrees of complexity [5–7]. These MSNs can function as encapsulation, protection and delivery agents and can be used in applications as diverse as medicine, foods, cosmetics and paints.

Curcumin is the main yellow bioactive component of Turmeric (*Curcuma longa*), a perennial plant of the ginger family (*Zingiberaceae*), native to the tropical South Asia [12]. It is chemically 1,7-bis (4-hydroxy-3-methoxyphenyl)-1,6-heptadiene-3,5-dione and extensively used as a spice, a food preservative and a coloring agent. Curcumin is non-toxic, highly promising natural antioxidant compound having a wide range of biological applications [13]. Curcumin is clinically well established to have no toxic effect even in 8 g/kg per day [14] and has medicinal properties including anti-inflammatory [15], anti-oxidant [16], antiamyloid [17], and anti-amyloid [18] activities. This molecule has fluorescence properties in the visible region, but the major limitation of curcumin is poor water solubility [19], degradation [20,21] and relatively poor quantum yield [22]. Interestingly, photophysical and excited state properties [23–31] of curcumin has attracted immense current research attention. Using curcumin as a molecular probe for solvent environment [32], micelle [33], proteins [34], liposomes [35,36] and microcapsules [37,38] have recently been realized. In this work, we prepare MSN loaded with curcumin. For the first

* Corresponding authors.
E-mail addresses: dp03@aub.edu.lb (D. Patra), jerosenh@abo.fi (J.M. Rosenholm).

http://dx.doi.org/10.1016/j.materresbull.2016.08.012
0025-5408/

time we have estimated polarizability inside the pores of the MSN, thus, the results establish the potential of a fluorescence probe based method for studying the environment inside the mesopores, which is critical since this cannot usually be easily reached using more conventional characterization methods. We also investigated influence of curcumin loading degree and surface functionalization on photophysical properties of curcumin loaded MSN.

2. Materials and methods

2.1. Synthesis of mesoporous silica nanoparticles

MCM-41 type mesoporous silica nanoparticles (MSN) were prepared by adding absolute ethanol (80 mL, 1.37 mol) to aqueous basic reaction solution with 20 v/v-% of reaction solution (320 mL deionized water, 17.78 mol). Cetyltrimethylammonium bromide (CTAB) (0.832 g, 5.8×10^{-3} mol) and tetraethylorthosilicate (TEOS) (4.2 mL, 18.72×10^{-3} mol) were mixed to the basic aqueous reaction solution as structure-directing agent (SDA) and silica source, respectively. The reaction was conducted at room temperature with stirring for overnight. The molar composition in synthesis solution was 949.8H_2O: 73.2 EtOH: 0.31 NaOH: 0.12 CTAB: 1 TEOS. The reagennts were added to reaction solution in the given order and TEOS, the silica precursor was added dropwise to reaction solution. After overnight reaction, the particles were collected by centrifugation. The SDA was removed by solvent extraction process with sonication for three times in ethanolic NH_4NO_3 solution (2 g NH_4NO_3/100 mL ethanol). The obtained particles were kept as dried powder after solvent extraction process.

2.2. Surface modification of mesoporous silica nanoparticles

To investigate the net surface charge effect on the fluorescent property of loaded curcumin on MSN, the surface modified MSN were synthesized with aminopropyltrimethoxysilane silane (APTMS) addition to the synthesis solution. For the synthesis, 360 g methanol was added to aqueous basic reaction solution (91 mg NaOH in 450 mL DI water). Cetyltrimethylammonium chloride (CTAC) (14.08 g), aminopropyltrimethoxysilane (0.155 mL) and tetramethylorthosilicate (TMOS) (1.152 mL) were mixed to the basic aqueous reaction solution dropwise with stirring. The reaction was conducted at room temperature with stirring overnight. The particles were collected by centrifugation and then the SDA was removed by solvent extraction process with sonication for three times in ethanolic NH_4NO_3 solution (2 g of NH_4NO_3 in 100 mL ethanol). The obtained particles were kept as dried powder after solvent extraction process. The synthesis mixture had a molar ratio of 0.9 TMOS: 0.1 APTMS: 1.27 CTAC: 0.26 NaOH: 1439 MeOH: 2560 H_2O. The sample was abbreviated as MSN-APTMS. The outer surface of MSN were modified by hyperbranching polymerization of aziridine which provides surface modified with hyperbranched poly(ethylene imine), PEI to provide high amount of amine group on the surface of MSN-APTMS. The amine functionalization was carried out by the method explained in our previous work given as the Supplementary information [39,40]. The sample was abbreviated as MSN-PEI. For further investigation of net surface charge effect on the fluorescent property of loaded curcumin on MSN, MSN-PEI sample was functionalized via either succinylation to yield negatively charged succinic acid groups (MSN-PEI-SUCC) or capping of the primary amines with uncharged acetyl groups (MSN-PEI-ACA). For both functionalization regimes, the PEI functionalized particles were dispersed in DMF, into which either succinic anhydride or acetic anhydride was added in excess then the reaction suspension was agitated overnight. Next day, the particles were separated by centrifugation, washed with absolute ethanol and vacuum dried for further experiments.

2.3. Curcumin loading on mesoporous silica nanoparticles

First of all, the adsorption isotherm of curcumin to the pristine MSN material was obtained. Here, 15 mg particles were dispersed in 10 mL of cyclohexane and increased amount of curcumin (0.1, 0.3, 0.5, 1, 5 w/w%) was added to the adsorption solutions. The suspensions were sonicated, stirred for overnight, centrifuged and washed with cyclohexane and finally curcumin loaded particles were dried in vacuum. For the surface modified samples the MSN-PEI, MSN-PEI-SUCC, MSN-PEI-ACA particles were dispersed in cyclohexane and curcumin loading was carried out at the concentration level of 0.3 w/w% and 1 w/w%.

2.4. Characterization of MSN material

The redispersibility and hydrodynamic particle size of dried MSN samples were determined by redispersing dried partilces in DI water and measuring by dynamic light scattering (DLS) (Malvern ZetaSizer NanoZS). Net surface charges of the produced MSNs in terms of zeta-potential were also determined by redispersing the particles in HEPES buffer (at pH 7.2, 25 mM) and measured by the same instrument in order to prove success of surface modifications via hyperbranched polymerization, succinilation and capping approaches. The morphology and non-agglomerated state of pristine MSN and MSN-APTMS were determined by Scanning electron microscopy (SEM; Jeol JSM-6335F). The structural parameters related to the mesoporosity (surface area, pore size and pore volume) of pristine MSN and MSN-APTMS were determined by nitrogen sorption measurements (Autosorb 1, Quantachrome). The porous structure and mesoscopic order of the nanoparticles were confirmed by transmission electron microscopy (FEI Tecnai 12 TEM (FEI Co., Hillsboro, OR, USA) operating at 120 kV and powder-XRD using a Kratky compact small-angle system (M. Braun). Thermogravimetric analysis (Netzsch TG 209) was utilized to determine the amount of hyperbranched amine groups (surface grafted PEI) on MSN sample at temperature intervals of 170 °C–770 °C.

2.5. Spectroscopic measurements

The adsorbed amount of curcumin was determined by UV–VIS spectrophotometer after eluting the adsorbed curcumin from MSN samples in ethanol at particle concentration of 0.5 mg/mL. The fluorescence intensity of curcumin loaded MSN suspensions were determined by fluorescence spectrometry (Perkin Elmer LS 50B, PerkinElmer) by dispersing them in DI water at 1.0, 0.5 and 0.25 mg/mL concentration. The spectra were recorded by excitation wavelength 425 nm for each sample and the intensity value for the emission was recorded for the highest peak point. For fluorescence investigation, the steady-state fluorescence spectra (excitation and emission) were recorded at room temperature using Jobin-Yvon-Horiba Fluorolog III fluorometer and the FluorEssence program where the excitation and emission slits width were 5 nm. The source of excitation was a 100 W Xenon lamp, and the used detector was R-928 operating at a voltage of 950 V.

3. Results and discussion

Mesoporous silica nanoparticles were synthesized as described in the materials and methods section. These nanoparticles were characterized by SEM (as shown in Fig. 1). The morphology of both pristine MSNs and MSN-APTMS were found to be spherical with a

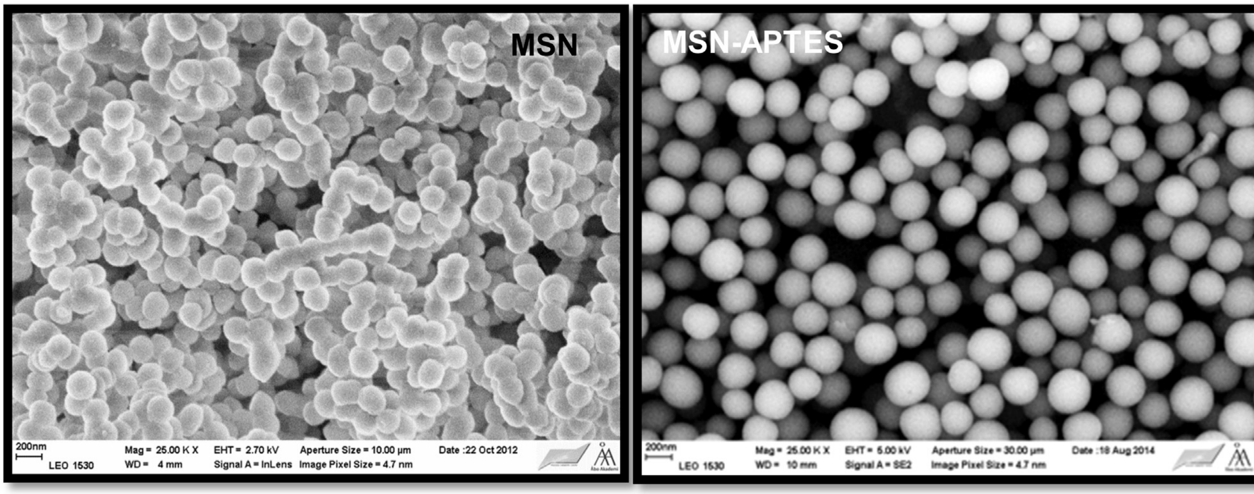

Fig. 1. Morphology of pristine MSN and APTES co-condensed MSN samples obtained from SEM.

Table 1
Hydrodynamic diameter and the zeta potential for the MSNs and modified MSNs samples.

SAMPLES	Hydrodynamic diameter [nm] in DI water	PDI	Zeta Potential [mv] in HEPES
MSN	546	0.27	−27
MSN-APTMS	539	0.15	22
MSN-PEI	314	0.2	59
MSN-PEI-SUCC	444	0.26	−59
MSN-PEI-ACA	1340	0.14	15

diameter of 200–300 nm. The hydrodynamic diameters of the particles are given in Table 1, which showed slightly higher values compared to the size obtained in SEM images. These results are rational as DLS generally gives exaggerated size values as compared to EM and thus we mainly use this as a characterization technique for determining the dispersability of the particles in solution. Amino-functionalized MSN-APTMS did not show any major difference in hydrodynamic diameter compared to pristine MSN, but the polydispersity value improved to 0.15, establishing that the degree of dispersability improved after modification of MSN with APTMS. However, the PEI functionalized mesoporous silica nanoparticles, MSN-PEI, showed a smaller hydrodynamic diameter than plain MSN, indicating good colloidal stability. Nevertheless, when the MSN-PEI were further functionalized via either succinylation to yield negatively charged succinic acid groups (MSN-PEI-SUCC) or capping of the primary amines with uncharged acetyl groups (MSN-PEI-ACA) the hydrodynamic diameter increased substantially; particularly, MSN-PEI-ACA formed large aggregates as also reflected in its hydrodynamic diameter. This should be related to its lower net surface charge (ζ-potential value) resulting from capping of the positively charged terminal amine groups with neutral acetyl groups.

The porosity, structural parameters related to the mesoporosity and mesoscopic ordering of nanoparticles were determined by TEM, powder X-ray diffraction analysis and N_2-sorption measurements (Fig. 2). Typical MCM-41 pore characteristics were observed

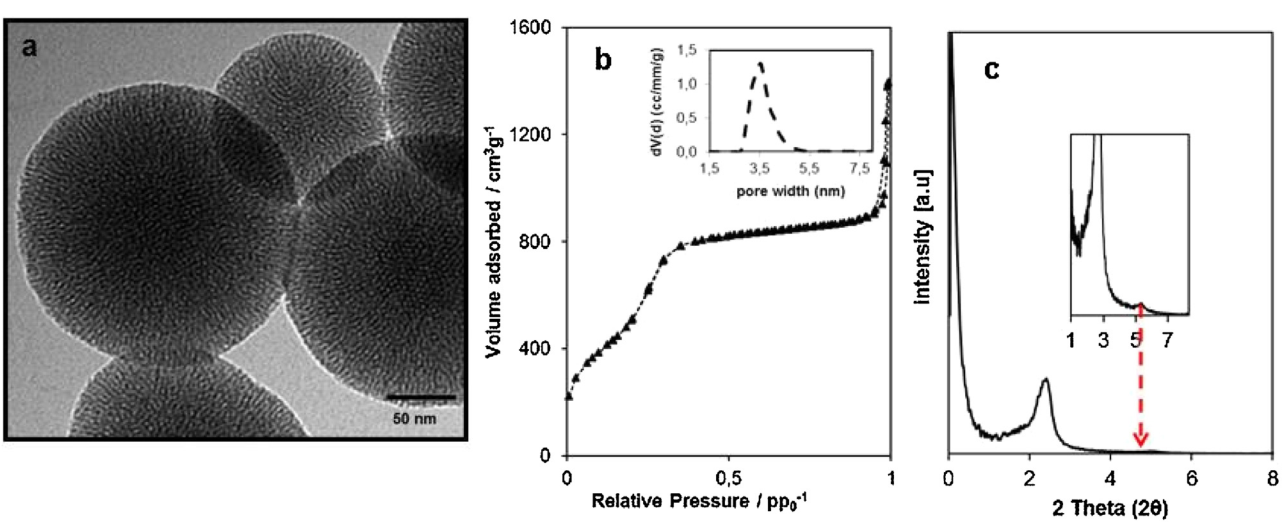

Fig. 2. a) TEM image b) N_2-sorption isotherm and pores size distribution c) powder X-ray diffraction pattern of pristine MSN.

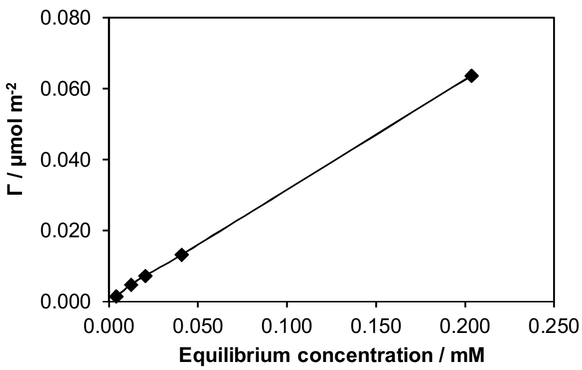

Fig. 3. The adsorption isotherm for curcumin loading to pristine MSN.

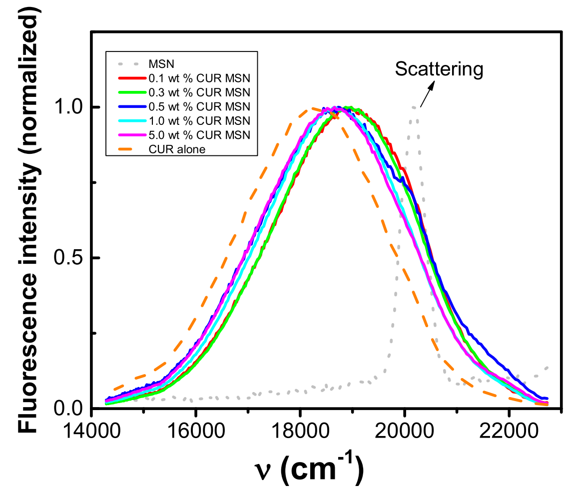

Fig. 4. Fluorescence spectra of curcumin loaded MSN-extracted particles. The excitation wavelength was 425 nm.

for the pristine MSN. In our reported case, MSNs had radially aligned pores (Fig. 2a) the average pore size value of MSN was as 3.2 nm (by Density functional theory (DFT)) and the BET surface area of pristine MSN was calculated as 1813 m^2/g. The particles had high degree of ordering as presented in Fig. 2c. The similar pore characteristic were also observed for MSN-APTMS, as presented in Fig. S1. TEM images shown in Fig. S2 also established preserved pore structure of MSN-PEI during hyperbranching polymerization process. The accumulated organic groups after hyperbranching polymerization of amine groups on MSN-PEI surface was calculated by thermogravimetric analysis, and estimated as 29 w% that resulted in +59 mV zeta potential value in HEPES pH 7.2. The same measurements for succinylated MSN-PEI (MSN-PEI-SUCC) and capped MSN-PEI (MSN-PEI-ACA) resulted in 35 w% and 37 w% organic groups on the surface of pristine MSN, respectively [41].

The adsorption isotherm for curcumin to the pristine MSN is shown in Fig. 3, which showed a linear dependency (i.e. Henry's adsorption isotherm). Table 2 summarizes the curcumin-loading efficacy for pristine MSNs, which was estimated by ethanol elution and UV–VIS spectrophotometric measurements, suggesting that complete adsorption took place. The fluorescence spectra of MSNs with different percentage of curcumin loading are shown in Fig. 4. The fluorescence maximum of 0.1% curcumin loaded MSNs extract was found at 18,975 cm^{-1}. The fluorescence maximum of free curcumin in water was obtained at 18,215 cm^{-1}. The shorter emission (longer wave number) of curcumin in MSNs extract illustrated a completely different microenvironment inside the pores of MSN by increasing the energy gap between the ground state and excited state. The fluorescence spectrum of curcumin is known to be sensitive to solvent polarity [32]. Theory of general solvent effects related the energy difference between ground and excited states with refractive index [42–44]. Increase in dielectric constant also stabilizes both the ground and excited states. Thus, the solvent environment can be expressed by measuring the polarizability (Δf):

$$(\Delta f) = \frac{\varepsilon - 1}{2\varepsilon + 1} - \frac{n^2 - 1}{2n^2 + 1}$$

Table 2
Curcumin-loading efficacy of MSN determined by ethanol elution and UV–vis spectrophotometric measurement.

Starting concentration of curcumin w/w%	Adsorbed Curcumin/MSN µg/mg
0.1	1.02
0.3	3.23
0.5	5.02
1	9.04
5	43.68

where ε and n are the dielectric constant and the index of refraction of the solvents, respectively. The fluorescence emission spectra of curcumin in few selective solvents are depicted in Fig. 5 and the corresponding plot for emission maximum vs. Δf is correlated in Fig. 6. There is a very good linear correlation between emission maximum of curcumin with polarizability of the solvent under investigation. Using this correlation, the estimated Δf inside the MSN is 0.32, which suggest a solvent environment close to that of methanol/ethanol.

However, the fluorescence maximum showed a red shift in wavelength (thus, blue shift in wave number scale) with increase in curcumin loading into the MSN as indicated in Fig. 7. The shift in the emission of maxima (in wave number scale) decreased from 0.1% loading to 1% loading of curcumin, after which it saturated. The shift in emission maximum is not due to change in solvent environment inside the pore; rather this can be explained based on the fact that as the concentration of curcumin increases inside the MSN pores, curcumin forms aggregates at higher concentration. Aggregation of fluorophores not only decreases the fluorescence intensity, but also decreases the energy gap between ground and excited states due to homo energy transfer.

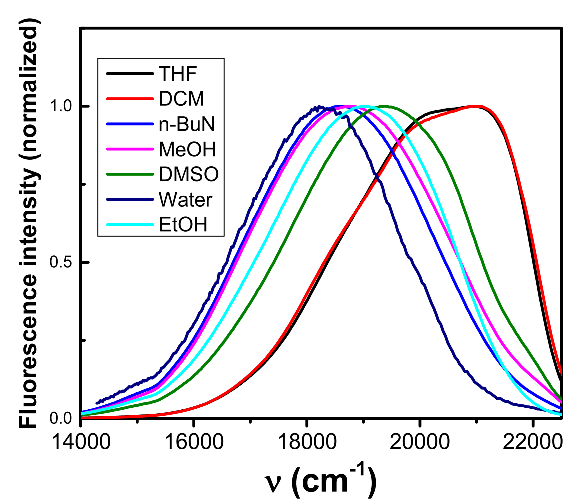

Fig. 5. Fluorescence spectra of curcumin in various solvents. The excitation wavelength was 425 nm.

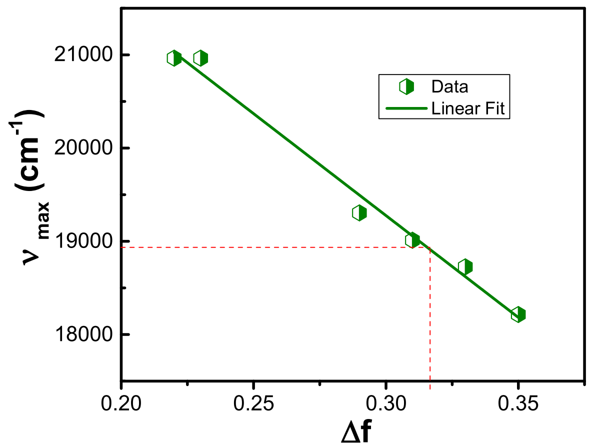

Fig. 6. Plot of emission maximum of curcumin in wave number (ν_{max} in cm^{-1}) vs. Δf.

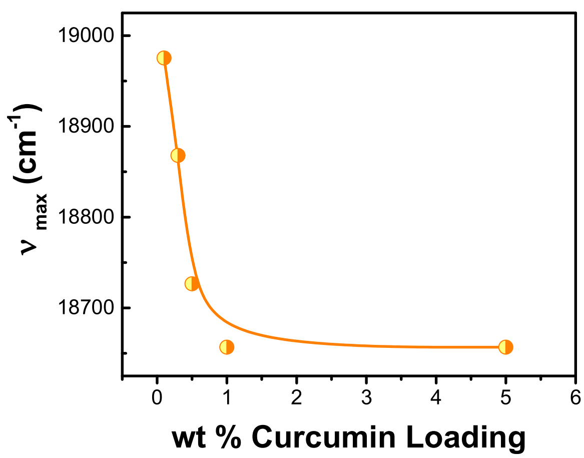

Fig. 7. Change in emission maximum of curcumin in wave number (ν_{max} in cm^{-1}) with loading of curcumin in pristine MSN.

The surface of the MSN was modified with PEI and further with succinic acid or acetic anhydride to diverse the net surface charges to understand the fluorescence response of curcumin. It was found that different surface chemistries, probably connected to the local accumulation of protons in the vicinity of the surface, remarkably influences fluorescence of loaded curcumin on MSN. The loaded curcumin amount for the different surface modified MSN are given in Table 3. As shown in Fig. 8, neutral net surface charge of charge-capped MSN-PEI-ACA gave rise to shorter wavelength emission, thus longer wave number scale, of curcumin compared to positive or negative net surface charge. The large energy gap between ground and excited states of curcumin in neutral net surface charge could be due to effect of pH on curcumin, This is further supported by our earlier observation [45] that the fluorescence of surface modified MSN are influenced by variation in local pH as opposed to surrounding pH. Large increase in fluorescence intensity of curcumin was observed for the MSN-PEI ACA which has net neutral surface charge compared to MSN-PEI/MSN-PEI-SUCC samples those have positive/negative net surface charge respectively (Fig. 9). The trend was similar for both 0.3% and 1% loading of curcumin, however, it should be noted that loading amount of curcumin did not influence appreciably the emission maximum of MSN-PEI, MSN-PEI-SUCC and MSN-PEI-ACA samples in contrast to found for uncapped MSN particles. This might be due to decrease in aggregation of curcumin in the presence of PEI, which is expected because of strong interaction between PEI and curcumin due to hydrophobic nature of curcumin. Here, it needs to be remembered that the zeta potential measurements (net surface charge) only determines the net charge in the slipping plane surrounding the outer particle surface, and cannot be expected to correlate directly with the degree of derivatization inside the pores. In the confined space of the mesopores, there is not much space for further derivatization after PEI surface hyperbranching polymerization as opposed to the non-constrained situation on the outer particle surface. Consequently, there can be expected to be a greater degree of non-functionalized terminal amine groups from the PEI layer inside on the pore surfaces, which may explain why the favorable

Table 3
Amount of curcumin loading on surface modified MSN.

Starting concentration of curcumin w/w%	Adsorbed Curcumin/MSNs µg/mg
MSN-PEI/CUR-0.3%	4.75
MSN-PEI/CUR-1%	8.75
MSN-PEI-SUC/CUR-0.3%	2.6
MSN-PEI-SUC/CUR-1%	9.42
MSN-PEI-ACA/CUR-0.3%	3.02
MSN-PEI-ACA/CUR 1%	13.15

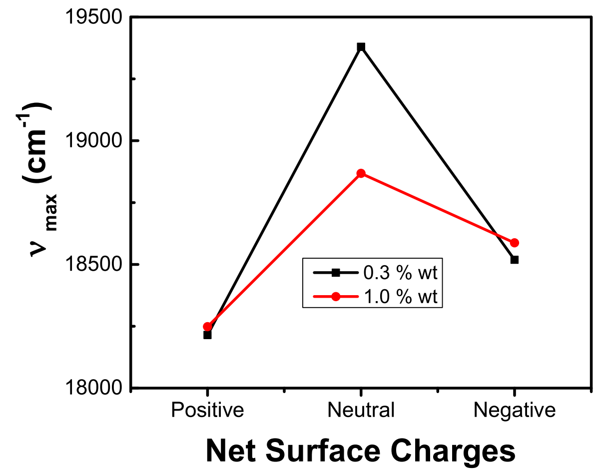

Fig. 8. Change in emission maximum of curcumin in wave number (ν_{max} in cm^{-1}) with loading on MSNs with different net surface charges on MSN-PEI (positive) MSN-PEI-ACA (neutral) and MSN-PEI-SUCC (negative).

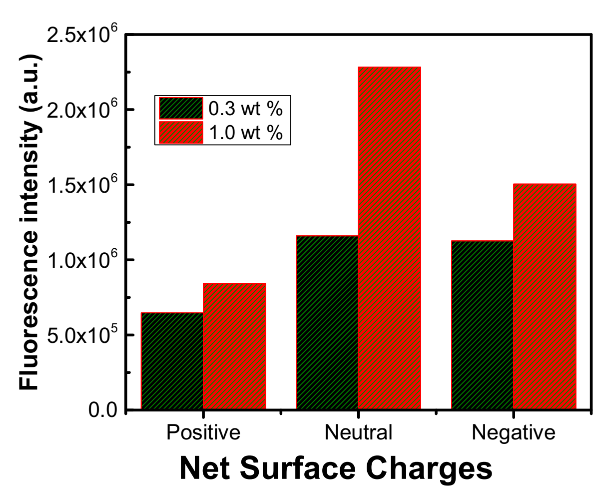

Fig. 9. Change in fluorescence intensity of curcumin loaded on MSNs with different net surface charges (MSN-PEI (positive) MSN-PEI-ACA (neutral) and MSN-PEI-SUCC (negative)).

effect of PEI interaction with curcumin (leading to lower degree of aggregation of curcumin molecules) can be observed in all three cases. However, the trend of surface functionalization effects on curcumin fluorescence is still evident (Figs. 8 and 9) which simultaneously highlights the potential of this method for studying the environment inside the mesopores, which is critical since this cannot usually be easily reached using more conventional characterization methods.

4. Conclusion

Various concentrations of curcumin could be successfully loaded onto the surface modified mesoporous silica nanoparticles. The polarizability inside the pores of the mesoporous silica nanoparticles was measured by using curcumin as a fluorescence probe. Polarizability value inside the pore was about 0.32, indicating a solvent environment similar to methanol/ethanol. However, increase in curcumin content inside the pore reduced the energy gap between ground and excited state that saturated at higher curcumin loading due to homo energy transfer between the molecules. Surface modification of mesoporous silica nanoparticles similarly influenced the spectral behavior of curcumin due to local accumulation of protons.

Acknowledgements

Financial support provided by American University of Beirut, Lebanon through Long-term development grants (DP), Academy of Finland project decision #260599 (DSK, DD, JMR) as well as Kamal A. Shair Central Research Science Laboratory (KAS CRSL) facilities to carry out this work is greatly acknowledged.

Appendix A. Supplementary data

Supplementary data associated with this article can be found, in the online version, at http://dx.doi.org/10.1016/j.materresbull.2016.08.012.

References

[1] C.T. Kresge, M.E. Leonowicz, W.J. Roth, J.C. Vartuli, Nature 359 (1992) 710.
[2] C. Argyo, V. Weiss, C. Bräuchle, T. Bein, Multifunctional mesoporous silica nanoparticles as a universal platform for drug delivery, Chem. Mater. 26 (1) (2014) 435–451.
[3] X.-L. Li, N. Hao, H.-Y. Chen, J.-J. Xu, Tumor marker mediated on demand drug release and real time monitoring system based on multi-functional mesoporous silica nanoparticles, Anal. Chem. 86 (20) (2014) 10239–10245.
[4] Z. Li, J.C. Barnes, A. Bosoy, J.F. Stoddart, J.I. Zink, Mesoporous silica nanoparticles in biomedical applications, Chem. Soc. Rev. 41 (7) (2012) 2590––2605.
[5] J.M. Rosenholm, A. Penninkangas, M. Linde 'n, Amino-functionalization of large-pore mesoscopically ordered silica by a one-step hyperbranching polymerization of a surface-grown polyethyleneimine, Chem. Commun. (2006) 3909–3911.
[6] E.P. Plueddemann, Silane Coupling Agents, Plenum, New York, 1991.
[7] A.S. Maria Chong, X.S. Zhao, J. Phys. Chem. B 107 (2003) 12650.
[8] X. Wang, K.S.K. Lin, J.C.C. Chan, S. Cheng, J. Phys. Chem. B 109 (2005) 1763.
[9] D.J. Macquarrie, D.B. Jackson, Chem. Commun. (1997) 1781.
[10] K.A. Utting, D.J. Macquarrie, New J. Chem. 24 (2000) 591.
[11] T. Yokoi, H. Yoshitake, T. Yamada, Y. Kubota, T. Tatsumi, J. Mater. Chem. 16 (2006) 1125.
[12] I. Chattopadhyay, et al., Turmeric and curcumin: biological actions and medicinal applications, Curr. Sci. 87 (2004) 44–53.
[13] A. Goel, A.B. Kunnumakkara, B.B. Aggarwal, Curcumin as curecumin: from kitchen to clinic, Biochem. Pharmacol. 75 (4) (2008) 787–809.
[14] A.L. Cheng, et al., Phase I clinical trial of curcumin, a chemopreventive agent, in patients with high-risk or pre-malignant lesions, Anticancer Res. 21 (2001) 2895–2900.
[15] J.T. Mague, W.L. Alworth, F.L. Payton, Curcumin and derivatives, Acta Cryst. C 60 (2004) 608––610.
[16] A. Khafif, S.P. Schantz, T.C. Chou, D. Edelstein, P.G. Sacks, Quantification of chemopreventive synergism between (-)-epigallocatechin-3-gallate and curcumin in normal, premalignant and malignant human oral epithelial cells, Carcinogenesis 19 (1998) 419–424.
[17] Y. Kiso, Y. Suzuki, N. Watanabe, Y. Oshima, H. Hikino, Antihepatotoxic principles of Curcuma longa rhizomes, Planta Med. 49 (1983) 185–187.
[18] F. Yang, G.P. Lim, A.N. Begum, O.J. Ubeda, M.R. Simmons, S.S. Ambegaokar, P. Chen, R. Kayed, C.G. Glabe, S.A. Frautschy, G.M. Cole, Curcumin inhibits formation of amyloid β oligomers and fibrils binds, plaques, and reduces amyloid in vivo, J. Biol. Chem. 280 (2004) 5892–5901.
[19] P. Anand, et al., Design of curcumin-loaded PLGA nanoparticles formulation with enhanced cellular uptake, and increased bioactivity in vitro and superior bioavailability in vivo, Mol. Pharm. 4 (2007) 807–818.
[20] M.H.M. Leung, H. Colangelo, T.W. Kee, Encapsulation of curcumin in cationic micelles suppresses alkaline hydrolysis, Langmuir 24 (2008) 5672–5675.
[21] L.C. Price, R.W. Buescher, Kinetics of alkaline degradation of the food pigments curcumin and curcuminoids, J. Food Sci. 62 (1997) 267–269.
[22] S.M. Khopde, et al., Effect of solvent on the excited-state photophysical properties of curcumin, Photochem. Photobiol. 72 (5) (2000) 625–631.
[23] S.V. Jovanovic, S. Steenken, C.W. Boone, M.G. Simic, H-atom transfer is a preferred antioxidant mechanism of curcumin, J. Am. Chem. Soc. 121 (1999) 9677–9681.
[24] L. Kong, K.I. Priyadarsini, H.-Y.I. Zhang, A theoretical investigation on intramolecular hydrogen-atom transfer in curcumin, J. Mol. Struct. 684 (2004) 111–116.
[25] L. Shen, H.-Y. Zhang, H.-F. Ji, Successful application of TD-DFT in transient absorption spectra assignment, Org. Lett. 7 (2) (2005) 243–246.
[26] C.R. Baiz, B.D. Dunietz, Theoretical studies of conjugation effects on excited state intramolecular hydrogen-atom transient reactions in model systems, J. Phys. Chem. A 111 (2007) 10139–10143.
[27] R. Adhikary, P. Mukherjee, T.W. Kee, J.W. Petrich, Excited state intramoleculr hydrogen atom transfer and solvation dynamics of the medicinal pigment curcumin, J. Phys. Chem. B 113 (2009) 5255–5261.
[28] R. Adhikary, P.J. Carlson, T.W. Kee, J.W. Petrich, Excited-state intramolecular hydrogen atom transfer of curcumin in surfactant micelles, J. Phys. Chem. B 114 (2010) 2997–3004.
[29] Y. Erez, I. Presiado, R. Gepshtein, D. Huppert, Temperature dependence of the fluorescence properties of curcumin, J. Phys. Chem. A 115 (2011) 10962–10971.
[30] C. Banerjee, C. Ghatak, S. Mandal, S. Ghosh, J. Kuchlyan, N. Sarkar, Curcumin in reverse micelle: an example to control excited-state intramolecular proton transfer (ESIPT) in confined media, J. Phys. Chem. B 117 (2013) 6906–6916.
[31] I. Presiado, Y. Erez, R. Gepshtein, N. Koifman, D. Huppert, Pressure effect on the excited-state proton transfer from curcumin to monols, J. Photochem. Photobiol. A Chem. 247 (2012) 42–51.
[32] (a) C.F. Chihnell, P. Bilski, K.J. Reszka, A.G. Motten, R.H. Sik, T.A. Dahl, Spectral and photochemical properties of curcumin, Photochem. Photobiol. 59 (1994) 295–302.
[33] D. Patra, C. Barakat, Unique role of ionic liquid [bmin] [BF4] during curcumin-surfactant association and micellization of cationic, anionic and non-ionic surfactant solutions, Spectrochim. Acta A Mol. Biomol. Spectrosc. 79 (2011) 1823–1828.
[34] C. Barakat, D. Patra, Combining time-resolved fluorescence technique with synchronous fluorescence spectroscopy to study bovine serum albumin-curcumin complex during unfolding and refolding processes, Luminescence 28 (2013) 149–155.
[35] E. El Khoury, D. Patra, Ionic liquid expedites partition of curcumin into solid gel but discourages into liquid crystalline phases of 1,2-dimyristoyl-sn-glycero-3-phosphocholine liposome, J. Phys. Chem. B 117 (2013) 9699–9708.
[36] D. Patra, E. El Khoury, D. Ahmadieh, S. Darwish, R.M. Tafech, Effect of curcumin on liposome: curcumin as a molecular probe for monitoring interaction of ionic liquids with 1,2-Dipalmitoyl-sn-Glycero-3-Phosphocholine liposome, Photochem. Photobiol. 88 (2012) 317–327.
[37] M. Mouslmani, D. Patra, Revoking excited state intra-molecular hydrogen transfer by size dependent tailor-made hierarchically ordered nanocapsules, RSC Adv. 4 (2014) 8317–8320.
[38] D. Patra, F. Sleem, A new method for pH triggered curcumin release by applying poly (L-lysine) mediated nanoparticle-congregation, Anal. Chim. Acta 795 (2013) 60––68.
[39] J.M. Rosenholm, A. Penninkangas, M. Lindén, Amino-functionalization of large-pore mesoscopically ordered silica by a one-step hyperbranching polymerization of a surface-grown polyethyleneimine, Chem. Commun. 37 (2006) 3909––3911.
[40] Jessica M. Rosenholm, Alain Duchanoy, Mika Lindén, Hyperbranching surface polymerization as a tool for preferential functionalization of the outer surface of mesoporous silica, Chem. Mater. 20 (2008) 1126–1133.
[41] D. Şen Karaman, D. Desai, R. Şenthilkumar, E.M. Johansson, N. Råtts, M. Odén, J. E. Eriksson, C. Sahlgren, D.M. Toivola, J.M. Rosenholm, Shape engineering vs organic modification of inorganic nanoparticles as a tool for enhancing cellular internalization, Nanoscale Res. Lett. 7 (2012) 358.
[42] N. Mataga, T. Kubota, Molecular Interactions of Electronic Spectra, Marcel Dekker, New York, 1970.
[43] W. Liptay, in: E.C. Lim (Ed.), Excited States, vol. I, Academic Press, New York, 1974, pp. 129––229.
[44] J.R. Lakowicz, Principles of Fluorescence Spectroscopy, Kluwer Academic, Plenum Publishers, New York, 1999.
[45] D. Desai, D.S. Karaman, N. Prabhakar, S. Tadayon, A. Duchanoy, D.M. Toivola, S. Rajpur, T. Näreoja, J.M. Rosenholm, Mesoporous Biomater. 1 (2014) 16–43.